π−π Interactions in Carbon Nanostructures

Journal:	*Chemical Society Reviews*
Manuscript ID:	CS-REV-07-2015-000578.R1
Article Type:	Tutorial Review
Date Submitted by the Author:	03-Aug-2015
Complete List of Authors:	Perez, Emilio; IMDEA Nanoscience, Martin, Nazario; Universidad Complutense de Madrid, Organic Chemistry Department; IMDEA nanoscience,

Journal Name

RSCPublishing

ARTICLE

π–π Interactions in Carbon Nanostructures

Emilio M. Pérez*[a] and Nazario Martín*[ab]

Cite this: DOI: 10.1039/x0xx00000x

Received 00th January 2012,
Accepted 00th January 2012

DOI: 10.1039/x0xx00000x

www.rsc.org/

π–π Interactions are the dominating supramolecular forces in systems like carbon nanostructures, which are inherently constituted by large conjugated π-systems. Their skilful use has allowed the construction of fascinating supramolecular ensembles, thus opening a new avenue in carbon chemistry. In this tutorial review, we provide a short introduction to carbon nanostructures, and show the basic concepts in π–π interactions involving fullerenes, carbon nanotubes, and graphene.

Key learning points:

1. The most prominent carbon nanostructures are fullerenes, carbon nanotubes, and graphene. Structure and chemical interconversion.
2. Van der Waals forces (particularly pi-pi interactions) and desolvation are the main factors that govern the supramolecular chemistry of carbon nanostructures.
3. Maximizing host-guest shape complementarity is the key to construct efficient receptors for fullerenes.
4. The supramolecular chemistry of carbon nanotubes is similar to that of fullerenes, but the relative importance of solvophobic interactions increases.
5. Planarity is not a prerequisite for the design of recognition motifs for graphene.

Introduction to Carbon Nanostructures

Carbon nanostructures are carbon allotropes with at least one dimension in the nanometer range. The most notable and extensively studied members of this family are fullerenes, carbon nanotubes, and graphene. All of these are composed solely of sp^2 hybridized carbon atoms, forming conjugated polycyclic structures of different size and shape. Fullerenes are closed carbon cages with spherical (C_{60} as the most abundant and stable) or elliptical shape (C_{70} and other giant fullerenes) and thus can be considered approximately 0D (zero dimensional), single-walled carbon nanotubes (SWNTs) are rolled-up seamless graphene cylinders (approximately 1D), and graphene which is strictly 2D since it is formed by one atom-thick flat sheets of carbon.

It is interesting to note that the above carbon nanoforms can transform into one another under certain conditions. As representative examples, graphene nanoribbons have been prepared by longitudinal unzipping of carbon nanotubes under harsh chemical conditions.[1, 2] Furthermore, in situ transmission electron microscopy (TEM) experiments have shown that graphene sheets undergo a direct transformation to fullerene cages under 80 keV electron beam irradiation.[3] Finally, fullerenes have been shown to convert to carbon nanotubes when encapsulated within other nanotubes and under correct stimulation, to form double-wall nanotubes.[4]

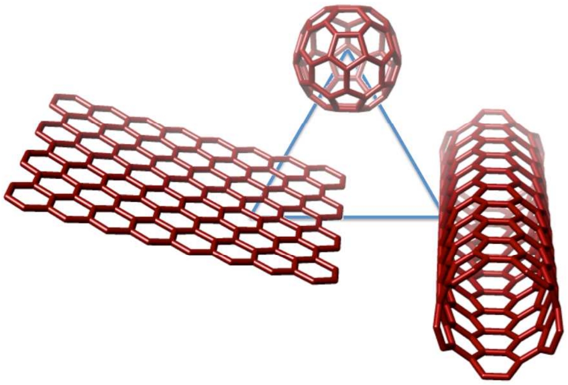

Figure 1. Representative nanoforms of carbon. From top to bottom: C_{60}, a fragment of graphene, and a SWNT. Their connection symbolizes their ability to transform between them.

The unique physical properties of these carbon nanostructures have made them the focus of intense research efforts in materials chemistry, in particular for their application in organic electronics.[5, 6] One of the key factors for their implementation in electronic devices is the control over the morphology of the device at the molecular level. To this end, it is mandatory to have a precise knowledge of the non-covalent forces that fullerenes, nanotubes, and graphene establish with other molecules, and themselves.

Introduction to the Noncovalent Chemistry of Carbon Nanoforms

There are several energetic factors to be considered when analyzing the nature of intermolecular interactions: i) van der Waals forces, ii) electrostatic interactions, iii) induction energy, iv) charge-transfer and v) desolvation.[7] Thanks to their solubility and precise molecular structure, the supramolecular association of fullerenes in solution has been studied quantitatively and intensively. This has allowed for discussions on the relative effects of each of these factors to the stability of the complexes. However, this is not possible with carbon nanotubes and graphene, where the lack of quantitative data (i.e. association constants) precludes discussions from a quantitative point of view. It is nevertheless an interesting exercise to analyse each one of them qualitatively with regards to the association of carbon nanoforms.

i) **Van der Waals forces:** these account for dispersion and repulsion forces, which are in essence dependent on the surface area available for interactions. Given their lack of functionality and their high surface to volume ratio, the supramolecular chemistry of carbon nanostructures is dominated by dispersion-type interactions.[7, 8]

A particular type of dispersion forces, π–π interactions play a most prominent role. The term π–π interactions refers to a subtype of dispersion forces established between unsaturated (poly)cyclic molecules. Despite being widely used and understood, some have argued against the use of expressions such as π–π interactions, π–stacking, etc., since saturated and unsaturated molecules of similar polarizability/size experience similar attractive forces.[9]

Nevertheless, supramolecular arrangements with aromatic moieties in close proximity (C-C distances typically around 3.5 Å, thus resembling the interlayer distances in graphite) are commonplace in both synthetic and natural systems,[10] and long-range π-stacking confers distinct properties to supramolecules, such as enhanced conductivity.[11] Moreover, Grimme has shown that genuine π-interactions take place between polycyclic unsaturated molecules with more than 10-15 carbon atoms.[12] We are in favour of the use of π–π interactions in general, and it seems particularly appropriate for the case of large conjugated systems such as carbon nanostructures. Nevertheless, it is always a safe option to stick to the more general terms van der Waals or dispersion forces.

ii) **Electrostatic interactions:** established between the static molecular charge distributions of the molecules involved. To a first approximation, and given the neutral and globally not polarized nature of carbon nanoforms, we can consider them largely unimportant. However, there is a very important exception to this, when significant charge-transfer occurs upon interaction with strong electron donors or (most commonly) acceptors (see below).

iii) **Induction energy:** defined as the interaction between the static charge distribution of one molecule and the induced charge distribution of the other. It is therefore only relevant for the case of charged molecules interacting with the carbon nanoforms. Although, due to their large surface area carbon nanoforms are polarizable species, the relevant parameter in terms of supramolecular interactions is the interaction energy per unit of surface area.[13] Induction should then only play a minor role in the overall stability of the complexes.

iv) **Charge-transfer:** charge-transfer bands are experimentally often found upon complexation of fullerenes with aromatic hosts, but it is generally accepted that these are more a spectroscopic result of the different supramolecular interactions than an interaction in themselves. With regards to the stability of the fullerene complexes in the ground state, we can safely deem charge-transfer interactions insignificant, or at least significantly smaller than dispersion forces.

Carbon nanotubes and graphene, on the other hand, can both accept and donate electrons to strong electron donors or acceptors, respectively. These charge-transfer processes can be substantial enough to result in the n or p-doping of the carbon nanostructure, which is reflected spectroscopically in a significant shift of the G band of its Raman spectrum. In these cases, charge-transfer interactions would result in the production of (partially) charged species, and consequently in relevant electrostatic interactions between them.

v) **Desolvation:** the intrinsic low solubility of carbon nanoforms in most common solvents directly translates into positive and quantitatively relevant solvophobic interactions.

Considering that there are only a few examples of supramolecular association of fullerene fragments, in this review, we will focus on supramolecular systems comprising fullerenes, SWNTs, and graphene. Other less-explored carbon nanoforms, such as endofullerenes, nanohorns, nanoonions, nanocups, nanotori, nanobuds, peapods, graphene quantum dots, etc. will also be omitted, although their supramolecular behaviour could fit within the aforementioned systems considered in this study (Figure 1).

Considering this is a tutorial review, we will try to provide the reader with the tools to maximize each of these contributions in order to control noncovalent interactions towards the formation of the desired supramolecular associates. Unfortunately, the reader must be warned that hardly any quantitative and comparable data are available for the cases of carbon nanotubes and graphene, so any discussions will be based on the qualitative observations reported.

Fullerenes

Maximize shape complementarity to maximize π–π interactions

Pristine fullerenes are unfunctionalized, approximately spherical polyenes. From the point of view of their supramolecular chemistry, this means that non-directional dispersion interactions will account for the vast majority of the binding energy in host-guest complexes. Since these forces depend directly on surface, the shape complementarity between host and guest becomes critical.[14] In this sense, distorted concave recognition motifs seem ideally suited for the association of the convex fullerenes. The importance of this shape complementarity is beautifully illustrated by the distortion from planarity observed in the solid state structure of some porphyrin-fullerene supramolecular complexes reported by Aida.[15] In the associate, the porphyrins adopt a non-planar concave conformation to maximize the positive interactions with the fullerene guest, even at the expense of some degree of conjugation (Figure 2). Interestingly, both the lateral alkyl chains as well as the coordination of the metal atom of the porphyrin (Zn, Rh, MeIr) to the two of the fullerene double bonds play an important role in the remarkably high binding constants (log K_a up to ~ 8) determined for these systems.

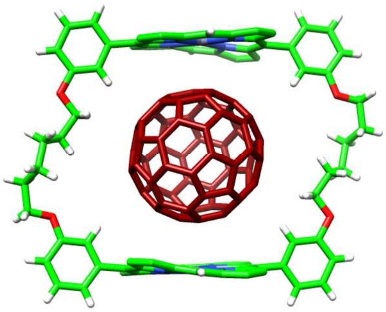

Figure 2. X-ray crystal structure of a bisporphyrin macrocycle•C_{60} inclusion complex, showing the distorted structure the porphyrins adopt to maximize interactions with C_{60}.[16] Ethyl substituents on the eigth β positions have been removed for clarity.

Besides the optimization of π–π interactions due to shape complementarity between concave hosts and convex fullerene guests, in 2006 Kawase and Kurata suggested that there might be an additional positive effect arising from the unsymmetrical nature of the π orbitals of the contorted molecules with respect to the convex (outer in the case of the fullerenes) and concave (inner in the case of the fullerene) sides. They termed this "concave-convex interaction".[17] Such interactions have been exploited in the synthesis of hosts based on curved recognition motifs, most prominently corannulene.[18] We have reported extensively on the ability of the curved electron donor (9,10-di(1,3-dithiol-2-ylidene)-9,10-dihydroanthracene, exTTF) to serve as a recognition motif for fullerenes. The geometric and electronic complementarity between the concave aromatic face of exTTF and the convex surface of the C_{60} was exploited to build very simple tweezers-like receptors which associate C_{60} with respectable binding constants in the order of log K_a = 3-4, in several solvents at room temperature.[19] Thanks to their synthetic accessibility, we could access a collection of hosts in which the specific contribution of concave-convex interactions to the molecular recognition of C_{60} was investigated. In particular, tweezers featuring exTTF, tetracyanoanthraquinone (TCAQ) and anthraquinone (AQ) as recognition motifs were synthesized (Figure 3). All three receptors bear the same number of aromatic rings and are approximately equal in size, so the contribution of π–π dispersion interactions can be considered equivalent. Both exTTF and TCAQ are concave recognition motifs, due to the steric repulsion between the anthracene core and the substituents in the 9,10 positions. They differ only in their electronic character, with exTTF being an electron donor and TCAQ an electron acceptor. Finally, AQ and TCAQ have similar electronic character, but AQ is completely flat. Unsurprisingly, the exTTF-based host shows the highest association constant, as π–π interactions are optimized due its concave shape, and charge-transfer interactions between exTTF and the electron acceptor C_{60} can further stabilize the associate. Remarkably, there is a noticeable difference between the binding affinities of the TCAQ and AQ tweezers that can be attributed to concave-convex interactions.[20]

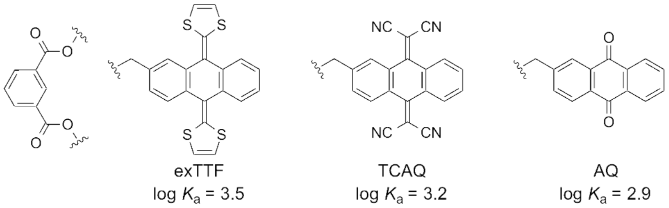

Figure 3. Chemical structure of the tweezers designed to measure the contribution of concave-convex interactions to the molecular recognition of C_{60}. Their association constants towards C_{60} in $CDCl_3/CS_2$ are also shown.[20] Note that the conjugated recognition motif is connected to the isophthalic ester spacer through a methylene linker in all cases.

Isobe and coworkers recently provided an extreme example of optimized π–π interaction between a fullerene guest and its host. They reported the inclusion of fullerenes in what they term a finite SWNT: a macrocycle formed by four units of the PAH anthranthrenylene, connected covalently with sufficient strain to bend the PAHs (Figure 4). Such macrocycle associates C_{60} and C_{70} with an outstanding log $K_a = 9.7 \pm 0.1$ and 9.6 ± 0.1 respectively in *o*-dichlorobenzene at room temperature.[21] That is, they show nanomolar affinity in an extremely competitive solvent! As revealed by analysis of the X-ray crystal structure of the complex, this tremendous affinity is due to the maximization of the dispersion interactions between host and guest. The PAH units are bent with an ideal curvature to complement the convex surface of C_{60}, establishing near-optimal π–π interactons (C-C distances < 3.4 Å). Moreover, the hexyl chains, initially introduced to enhance solubility, also interact with the fullerene, fully covering its surface and compensating for the desolvation penalty.

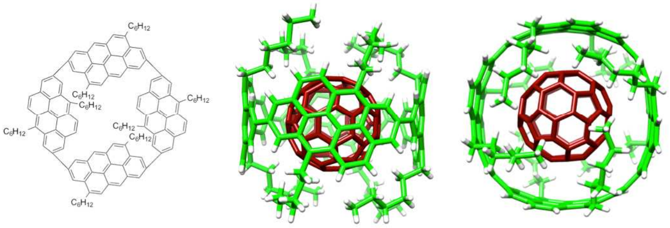

Figure 4. Chemical structure of the finite SWNT reported by Isobe, and the solid-state structure of its C_{60} inclusion complex.[21]

All these examples of association in solution illustrate the main take-home message: the most important part of designing hosts for fullerenes is to maximize shape complementarity between the host and the fullerene guest. In fact, even very small changes in the structure of the host that affect exclusively the shape complementarity result in several orders of magnitude of variation of the association constant.[22] In a lighter vein, we could say that, when it comes to designing hosts for fullerenes, one size fits ball. The good news is that, based on our experience,[22] simple molecular mechanics calculations are very useful to anticipate if our receptor is a good match for the fullerene we would like to associate.

Solvophobic effects and thermodynamic considerations

As we have already mentioned, elestrostatic interactions, induction and charge-transfer are usually only minor contributions to the total association energy. Therefore, second in relative importance to maximizing van der Waals interactions are (de)solvation effects in. In this sense, the low solubility of fullerenes in most organic solvents directly translates into significant and positive solvophobic interactions. This will obviously be in our favour with regards to obtaining large association constants. A few years ago, the groups of Armaroli, Reed, and Boyd described how the association of calix[4]arene-linked bisporphyrin tweezers was affected by changes in the solvent. For their investigation, they used cyclohexane, benzonitrile, dichloromethane, toluene and toluene/acetonitrile mixtures.[23] They found an inverse correlation between the stability of the complex and the solubility of the fullerene (Figure 5).

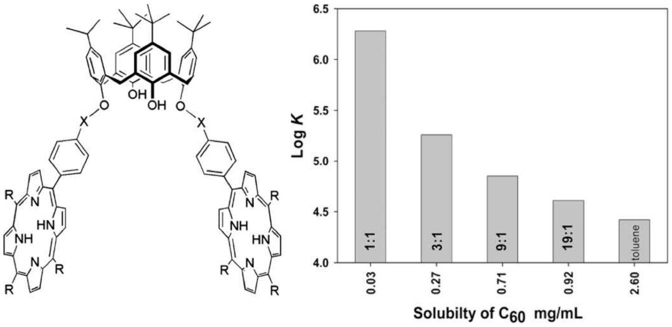

Figure 5. General structure of the calix[4]arene-linked bisporphyrin tweezers and relationship between the log Ka and the solubility of C_{60} in toluene/acetonitrile mixtures. Adapted with permission from ref. [23]. Copyright (2006) American Chemical Society.

More recently, Sygula, Lewis, and coworkers have reported on the thermodynamics of association of “buckycatcher” as investigated through ITC and NMR titrations in toluene, chlorobenzene, and *o*-dichlorobenzene, reaching the same conclusion: association constants increase with decreasing solubility.[24]

For both the calix[4]arene-linked bisporphyrin tweezers and the corannulene “buckycatcher” the relative weight of the enthalpic and entropic factors behind the association of fullerenes was also investigated.[23, 24] The findings of both teams are similar: generally speaking, the association process is enthalpically driven, with significantly smaller entropic contributions. We have also reached similar conclusions with regards to exTTF macrocycles.[22] These results emphasize once again the importance of maximizing positive dispersion interactions in the design of the fullerene host, which will be the main contribution to the enthalpic stabilization of the complex.

From host-guest chemistry to materials science

One of the main driving forces behind the interest in the noncovalent chemistry of fullerenes is the self-assembly of fullerene-based supramolecular materials.[25] When the host-guest chemistry is sufficiently fine-tuned, $\pi-\pi$ interactions can be employed in the construction of fullerene-based polymeric materials. For instance, Haino and co-workers have recently described linear supramolecular polymers and 3D networks based on the molecular recognition between calix[5]arene and C_{60} (Figure 6).[26] To that end, the Japanese team synthesized di- and tritopic calixarene hosts, and studied their association to form polymers through a variety of techniques, including NMR, absorption and fluorescence spectroscopy, SEM and AFM.

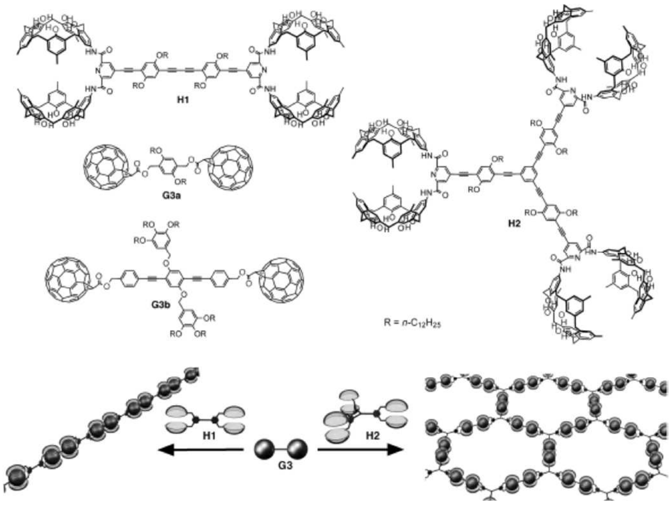

Figure 6. Chemical structure of the calixarene-based hosts and fullerene guest described by Haino and co-workers. Adapted with permission from ref. [26]. Copyright (2014) John Wiley & Sons.

The relevance of a correct shape match between host and guest is once more highlighted in the synthesis of a supramolecular polymer with outstanding degree of polymerization based on the interaction between a C_{60} fragment and an exTTF-based macrocycle (Figure 7).[27] Thanks to the preorganization in the host part,[22] a remarkable log $K_a = 5.1 \pm 0.5$ was found for the model host-guest couple in $CHCl_3$ at room temperature. In accordance with the large binding constant, the monomer self-assembles with a very high degree of polymerization, reaching MW well above 100 kDa in solution. Remarkably we could directly detect polymers of up to 90 kDa in the gas phase through MALDI-TOF spectrometry.

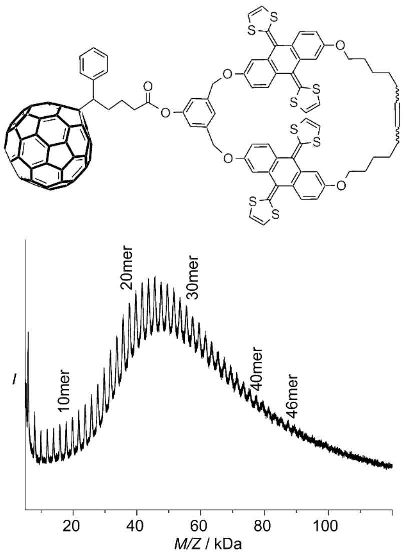

Figure 7. Chemical structure of the exTTF-C_{60} monomer and MALDI-TOF spectrum, showing its high degree of polymerization.[27]

Carbon nanotubes

SWNTs are rolled-up graphene sheets, forming tubules of diameter typically around 1 nm. Their extraordinary physical properties have made them one of the most intensely researched nanomaterials.[28] Their supramolecular chemistry has attracted a lot of attention, but despite well over a decade of research, to date there is no standard method for the determination of association constants towards SWNTs. This is mainly due to the heterogeneous structure of the SWNTs and their characteristic insolubility, which makes it impossible to determine the molar concentration of SWNTs in solution. The lack of quantitative and comparable experimental data unfortunately prevents an in-depth discussion of the factors governing the supramolecular association of SWNTs. A significant effort from the theoretical community has helped to partially compensate for this lack of experimental data,[29] but *in silico* experiments are usually performed in the gas phase, where solvophobic interactions are not considered. From a purely qualitative point of view, SWNTs are structurally very similar to fullerenes, so it is safe to assume that the same main principles apply, and most supramolecular complexes will be based on an optimization of the dispersion interactions with the nanotube surface.

The main difference between fullerenes and SWNTs is the extreme aspect ratio of the latter, which makes them particularly eager to interact with themselves, forming insoluble aggregates. This insolubility in turn enhances solvophobic interactions, so that surfactants, proteins, oligonucleotides, polymers, etc. in which the role of π–π interactions is not obvious successfully form non-covalent hybrids with SWNTs.[29, 30]

Here, we will focus only on supramolecular associates of SWNTs where the main interaction is π–stacking. And we shall start at the very beginning, with Dai's[31] and Nakashima's pioneering work on pyrene. The Stanford group utilized the succinimidyl ester of 1-pyrenebutanoic acid (Figure 8a) to attach biomolecules of interest in a two-step process. They first adsorbed the pyrene derivative onto the walls of the SWNTs through π–π interactions, and then reacted it with terminal amines in the protein to form the corresponding amides. Using 1-(trimethylammonium-acetyl)pyrene (Figure 8b), a water soluble salt of pyrene, Nakashima's team was able to disperse SWNTs in water for the first time.[32] Later, many other groups have used pyrene as an anchor to attach a variety of molecules of interest to the sidewalls of SWNTs.[30]

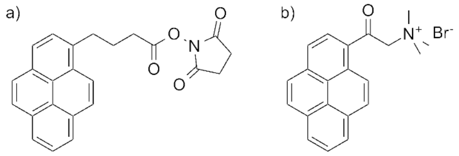

Figure 8. a) Pyrene bearing an activated ester, used by Dai and co-workers to immobilize proteins onto SWNTs.[31] b) Water soluble pyrene salt used by Nakashima and co-workers to disperse SWNTs in water.[32]

The chiral indices of SWNT determine their chirality, diameter, and electronic properties. Most samples of SWNT are composed of a complicated mixture of nanotubes. The separation of SWNTs through selective association according to their chirality is a phenomenal challenge from both the fundamental and applied point of view. The first degree of discrimination is to achieve diameter selectivity. This has been achieved with a variety of systems.[8] A further degree of complexity arises if one considers that each nanotube chirality is produced as an enantiomeric pair of nanotubes with opposite helicity. In one of the most significant achievements in the supramolecular chemistry of SWNTs, Komatsu and co-workers achieved the selective extraction of optically active nanotubes utilizing the chiral bisporphyrin tweezers shown in Figure 9. The rigid structure of the porphyrin tweezers allows them to discriminate between nanotubes of different chiral indices (i.e. diameter) while the addition of chiral centres at the substituents of the porphyrins make them selective between enantiomers of single-chirality SWNTs. Indeed, upon extraction of a methanol suspension of a commercial sample of CoMoCAT SWNTs with either (*R*) or (*S*) enantiomers of the tweezers, followed by centrifugation and removal of the host molecules, there is a considerable enrichment in opposite enantiomers of the (6, 5) SWNT, as demonstrated through CD measurements.[33] By comparing with results from density gradient ultracentrifugation, the authors estimated a remarkable 67 % ee.

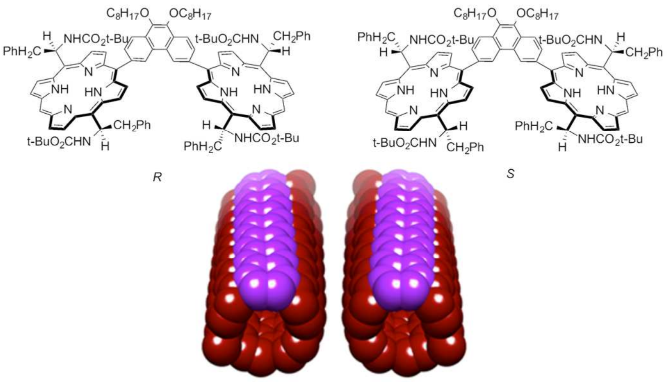

Figure 9. Top: Chemical structure of the *R* and *S* enantiomers of the chiral bisporphyrin tweezers used by Komatsu and co-workers to achieve diameter and chirality selective extraction of SWNTs. Bottom: *M* and *P* (6, 5) SWNTs. Adapted with permission from ref. [8]. Copyright (2012) the Royal Society of Chemistry.

One of the most appealing cases of supramolecular chemistry of carbon nanotubes is their interaction with the nucleotides, in which π–π interactions with the nucleobases is thought to play a major role.[34] For example, DNA has been shown to bind to SWNTs in a sequence-specific manner, which was skilfully exploited for the purification of SWNTs according to their chirality.[35] More recently, Vezenov, Jagota and co-workers have obtained experimental data quantifying the strenght of the interaction between the different nucleobases and SWNTs, using single strand DNA (ss-DNA) and AFM techniques (Figure 10).[36] Their results show adenine interaction is slightly stronger (ca. −1.7 kcal mol^{-1}), than that of guanine, thymine and cytosine (ca. −1.3 kcal mol^{-1}).

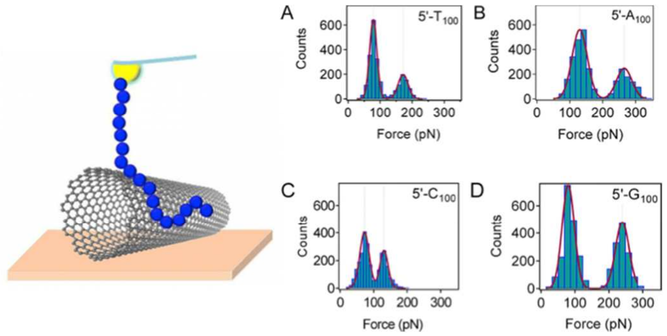

Figure 10. Left: cartoon representation of the AFM setup used to measure interactions between nucleobases and ss-DNA.. Right: statistical distribution of forces obtained for the different nucleobases. Adapted with permission from ref. 36. Copyright (2014) the American Chemical Society.

Pyrene, porphyrins and nucleobases are all planar, so that there is a flat-convex mismatch with the surface of SWNTs. Indeed, it has been shown that the affinity of pyrene for SWNTs increases with the nanotube diameter, that is, as its surface becomes closer to planarity.[37] One would therefore expect that aromatic systems with the right curvature would establish even more effective π–π interactions with SWNTs. Although quantitative comparison between different recognition motifs for SWNTs is difficult, we have indeed shown that both curved electron donors such as exTTF[38] and acceptors such as TCAQ[39] are valid recognition motifs for SWNTs.

Recently, we have succeeded in exploiting the exTTF-SWNT interaction to template the formation of mechanically interlocked derivatives of SWNTs (MINTs) for the first time.[40,41] To do so, we relied on a clipping strategy in which molecules featuring two SWNT-recognition units associate with the nanotubes supramolecularly, templating the cyclization around the SWNTs via ring closing metathesis (RCM), as depicted schematically in Figure 11a. The macrocycle's cavity is sufficiently large to accommodate SWNTs of diameter around 1 nm (Figure 11b). A very thorough collection of spectroscopic and analytical techniques, together with adequate control experiments, demonstrated the interlocked nature of MINTs. Moreover, we were able to visualize individual macrocycles wrapped around the SWNTs through HR-STEM (Figure 11c).

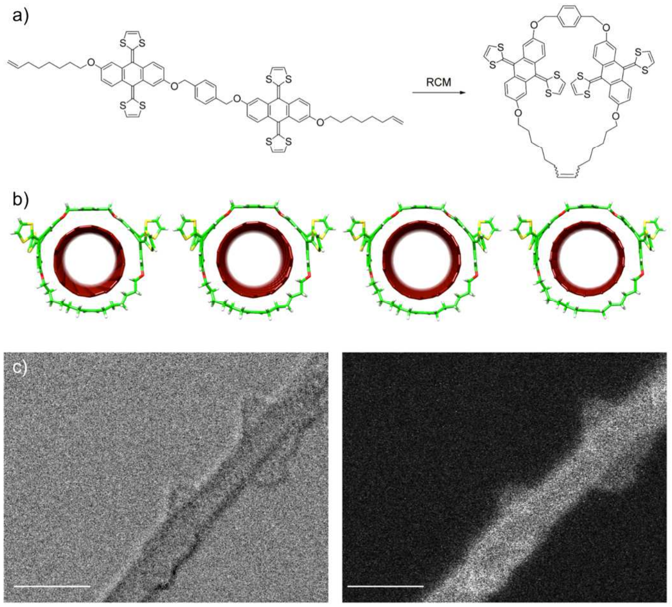

Figure 11. a) Structure of the linear bis-exTTF precursor for the formation of MINTs via RCM. b) Energy minimized models (MMFF94) of MINTs featuring, from left to right: (7,6), (9,4), (11,3) and (13,0) SWNTs, all of which show significant positive interactions with the macrocycle. c) Bright field (left) and dark-field (right) HR-STEM images of MINTs. Adapted with permission from ref. [40]. Copyright (2014) John Wiley & Sons.

Later, we have also proven that planar recognition motifs, such as pyrene can also template the formation of MINTs.[42] However, in this case the yield for MINT formation is slightly lower, which can be considered an indirect indication that the better shape complementarity of exTTF does indeed result in more efficient π–π interactions.

Graphene

Graphene is a single layer of sp^2-hybridized carbon atoms arranged in a honeycomb pattern. Considering its structure, its chemistry is very similar to that of SWNTs, although the lack of curvature makes it less reactive in terms of covalent chemistry and even more prone to establish strong van der

Waals and π–π interactions.[43] In fact, nearly any small molecule can adsorb onto graphene, which endows it with an extreme sensitivity for the construction of sensors, down to the single molecule.[44] Unfortunately, and for the same reason, this outstanding sensitivity is coupled to a remarkable lack of selectivity.

Graphite is the most obvious example of π–π interactions between graphene layers. Unsurprisingly, PAHs and their derivatives are the most widely used binding motifs for graphene. Using a cobalt complex as an electrochemical label, Dichtel, Abruña and co-workers have shown that the trispyrene derivative shown in Figure 12 adsorbs on graphene very strongly, with a remarkable $\Delta G_{\mathrm{ads}} = -38.8 \pm 0.2$ kJ mol^{-1}.[45] Interestingly, a structural analogue bearing one pyrene unit only, showed nearly identical $\Delta G_{\mathrm{ads}} = -38.3 \pm 0.5$ kJ mol^{-1}. This surprising result was explained by hypothesizing that pyrene-pyrene intramolecular interactions present in the tripod are lost upon adsorption, incurring in an energetic penalty with respect to the monovalent pyrene derivative. Nevertheless, once the adsorbate is formed, the trispyrene derivative shows much larger kinetic stability, desorbing over 1000 times more slowly than the monovalent one.

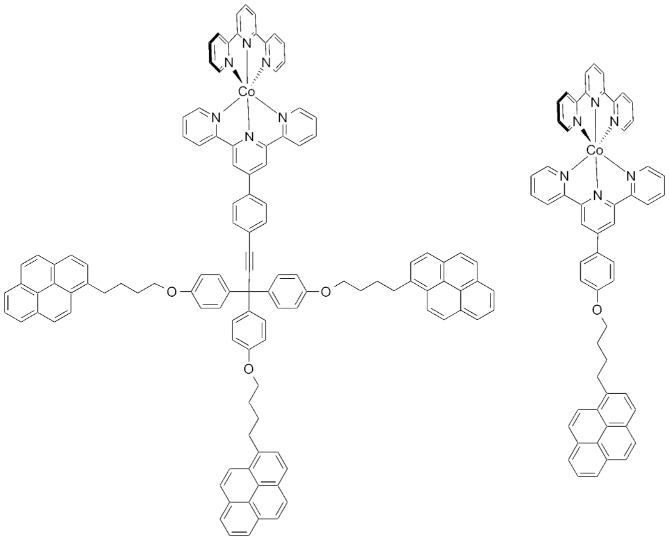

Figure 12. Trispyrene derivative described by the groups of Abruña and Dichtel.[45]

Perylene bisimides (PBIs), are industrially relevant chromophores with outstanding otpical properties. Their planar perylene core makes them ideal candidates to establish strong π–π stacking interactions with graphene. A few years ago, Hirsch et al. reported the supramolecular association of PBIs with a graphene dispersion in NMP (Figure 13).

The strong fluorescence of PBI was nearly completely quenched upon interaction with graphene, confirming a strong electronic communication between the cromophore and graphene.[46]

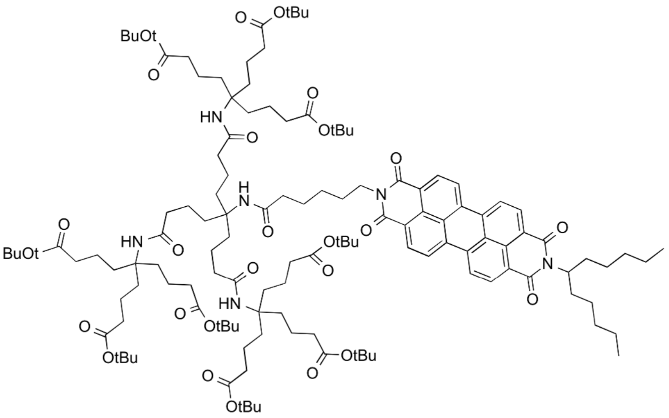

Figure 13. Chemical structure of the PBI dendronized derivative shown by Hirsch et al. to associate graphene in solution.[46]

Even though planar PAHs are the most obvious supramolecular partners for graphene, we have shown that planarity is not a prerequisite for graphene binding motifs.[47] In particular, we used gold nanoparticles decorated with multiple units of exTTF (Figure 15) to prove that a multivalent approach can be used to produce graphene supramolecular composites even with nonplanar binding motifs. Several approaches between exTTF and graphene were found to be energetically favourable through DFT calculations. The energetic stabilization arises from a combination of CH–π and π–π interactions. Scrutiny under TEM of a mixture of previously exfoliated graphene and the exTTF gold nanoparticles showed that the basal planes of graphene were heavily functionalized with nanoparticles. A closer examination of the micrographs suggested that the nanoparticles maximize their non-covalent interactions by localizing preferentially between layers of graphene.

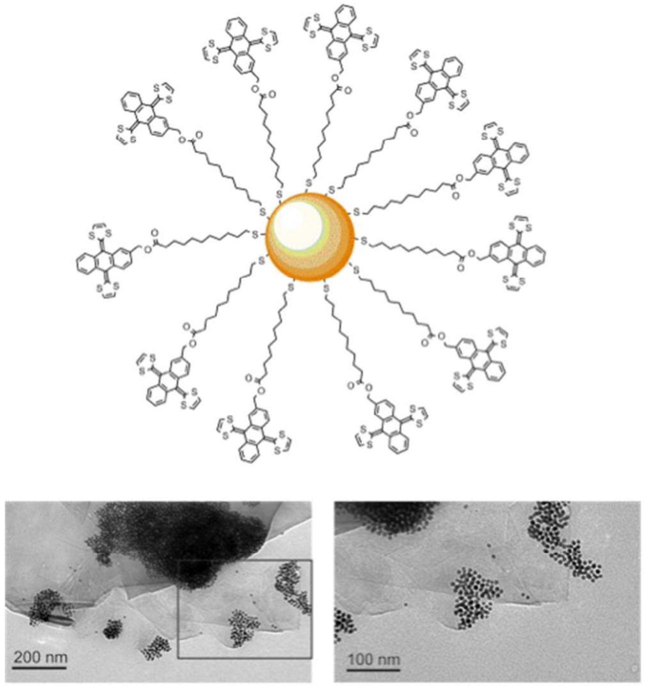

Figure 13. Cartoon showing the structure of the exTTF-decorated gold nanoparticles (up) and TEM images showing their intercalation between graphene layers (down). Adapted with permission from ref. [47]. Copyright (2013) John Wiley & Sons.

It has also been shown that porphyrins bearing bulky mesityl groups in the meso positions, which would be expected to prevent adequate π-stacking, are able to attach to graphene in a supramolecular fashion. In fact, the association is sufficient to enhance the yield of exfoliation from graphite by up to 140%.[48] These results show that, at least in the case of graphene, π–π interactions are not necessarily dominant with respect to other dispersion-type forces.

Conclusions

Carbon nanostructures are at the forefront in current science due to their expected applications in a variety of fields. Since the discovery of [60]fullerene as a new third allotropic form of carbon thirty years ago, a wide variety of other new carbon nanostructures has followed, thus giving rise to a new multidisciplinar area of study ranging from the synthesis of new nanoforms of carbon to the search for potential applications.

In this tutorial review we have shown the basic concepts in π–π interactions involving carbon nanostructures. In particular, we have focused on the supramolecular chemistry of fullerenes, SWNTs and graphene.

In the case of fullerenes, thanks to the generalized determination of quantitative K_a data, analysis of the literature allows for relatively clear conclusions with regards to their noncovalent chemistry: hosts for fullerenes should be designed considering a maximization of contact surface area between host and guest (i.e. dispersion forces) as the main parameter. Besides this, solvophobic interactions are also relatively straightforward to control, as a decrease in solubility of the fullerene directly results in an increase of the association constant.

Unfortunately, the heterogeneous nature of SWNTs and graphene samples has prevented the production of quantitative and comparable data so it is difficult to be as convincing with regards to their noncovalent chemistry. However, based on the examples described here, we can extract a couple of common points. The insolubility and extreme aspect ratio of both SWNTs and graphene make them particularly prone to establish strong noncovalent interactions with a variety of molecules. While for SWNTs shape complementarity seems to enhance π–π interactions, in the case of graphene experimental data show that it is not a prerequisite, and that other dispersion forces might be at least as important.

Our final goal in this tutorial review is, therefore, to help the non-specialized readership to have a better understanding of the importance of the π–π interactions as a dominating force in the realm of carbon nanostructures, and their balance with other weak non-covalent interactions. The existence of π–π interactions as dominating supramolecular forces in all carbon nanostructures represents an important basic concept, which must be taken into account when approaching the supramolecular chemistry of the carbon nanoforms known to date, but also of those still underexplored, such as fullerene fragments.[49, 50]

Acknowledgements

Financial support by the European Research Council (StG-307609-MINT and AdG-ERC-320441-Chirallcarbon), Ministerio de Economía y Competitividad (MINECO) of Spain (CTQ2011-25714 and CTQ2011-24652), the Comunidad Autónoma de Madrid (PHOTOCARBON project S2013/MIT-2841), MOLESCO (grant number 606728) is greatly appreciated. N. M. is indebted to Alexander von Humboldt Foundation.

Notes and references

[a] IMDEA Nanociencia, C/ Faraday 9, Ciudad Universitaria de Cantoblanco, 28049, Madrid, Spain. E-mail: emilio.perez@imdea.org

[b] Departamento de Química Orgánica, Fac. C.C. Químicas, Universidad Complutense de Madrid, Av. Complutense s/n, E-28040 Madrid, Spain. Fax: (+)34 913944103; E-mail: nazmar@ucm.es

1. D. V. Kosynkin, A. L. Higginbotham, A. Sinitskii, J. R. Lomeda, A. Dimiev, B. K. Price and J. M. Tour, *Nature*, 2009, **458**, 872-876.
2. L. Jiao, L. Zhang, X. Wang, G. Diankov and H. Dai, *Nature*, 2009, **458**, 877-880.
3. A. Chuvilin, U. Kaiser, E. Bichoutskaia, N. A. Besley and A. N. Khlobystov, *Nat. Chem.*, 2010, **2**, 450-453.
4. S. Bandow, M. Takizawa, K. Hirahara, M. Yudasaka and S. Iijima, *Chem. Phys. Lett.*, 2001, **337**, 48-54.
5. M. J. Allen, V. C. Tung and R. B. Kaner, *Chem. Rev.*, 2010, **110**, 132-145, and references therein.
6. J. L. Delgado, P.-A. Bouit, S. Filippone, M. A. Herranz and N. Martín, *Chem. Commun.*, 2010, **46**, 4853-4865, and references therein.
7. E. M. Pérez and N. Martín, *Chem. Soc. Rev.*, 2008, **37**, 1512-1519, and references therein.
8. E. M. Pérez and N. Martín, *Org. Biomol. Chem.*, 2012, **10**, 3577-3583, and references therein.
9. C. R. Martínez and B. L. Iverson, *Chem. Sci.*, 2012, **3**, 2191-2201.
10. L. M. Salonen, M. Ellermann and F. Diederich, *Angew. Chem., Int. Ed.*, 2011, **50**, 4808-4842, and references therein.
11. M. R. Wasielewski, *Acc. Chem. Res.*, 2009, **42**, 1910-1921, and references therein.
12. S. Grimme, *Angew. Chem., Int. Ed.*, 2008, **47**, 3430-3434.
13. C. A. Hunter, *Angew. Chem., Int. Ed.*, 2004, **43**, 5310-5324.
14. D. Canevet, E. M. Pérez and N. Martín, *Angew. Chem., Int. Ed. Engl.*, 2011, **50**, 9248-9259, and references therein.

15. K. Tashiro and T. Aida, *Chem. Soc. Rev.*, 2007, **36**, 189-197, and references therein.
16. J.-Y. Zheng, K. Tashiro, Y. Hirabayashi, K. Kinbara, K. Saigo, T. Aida, S. Sakamoto and K. Yamaguchi, *Angew. Chem., Int. Ed.*, 2001, **40**, 1857-1861.
17. T. Kawase and H. Kurata, *Chem. Rev.*, 2006, **106**, 5250-5273, and references therein.
18. A. Sygula, F. R. Fronczek, R. Sygula, P. W. Rabideau and M. M. Olmstead, *J. Am. Chem. Soc.*, 2007, **129**, 3842-3843.
19. E. M. Pérez, B. M. Illescas, M. A. Herranz and N. Martín, *New J. Chem.*, 2009, **33**, 228-234, and references therein.
20. E. M. Pérez, A. L. Capodilupo, G. Fernández, L. Sánchez, P. M. Viruela, R. Viruela, E. Ortí, M. Bietti and N. Martín, *Chem. Commun.*, 2008, 4567-4569.
21. T. Matsuno, S. Sato, R. Iizuka and H. Isobe, *Chem. Sci.*, 2015, **6**, 909-916.
22. D. Canevet, M. Gallego, H. Isla, A. de Juan, E. M. Pérez and N. Martín, *J. Am. Chem. Soc.*, 2011, **133**, 3184-3190.
23. A. Hosseini, S. Taylor, G. Accorsi, N. Armaroli, C. A. Reed and P. D. W. Boyd, *J. Am. Chem. Soc.*, 2006, **128**, 15903-15913.
24. V. H. Le, M. Yanney, M. McGuire, A. Sygula and E. A. Lewis, *J. Phys. Chem. B*, 2014, **118**, 11956-11964.
25. T. Nakanishi, *Chem. Commun.*, 2010, **46**, 3425-3436, and references therein.
26. T. Hirao, M. Tosaka, S. Yamago and T. Haino, *Chem. Eur. J.*, 2014, **20**, 16138-16146.
27. H. Isla, E. M. Pérez and N. Martín, *Angew. Chem., Int. Ed.*, 2014, **53**, 5629-5633.
28. J. M. Schnorr and T. M. Swager, *Chem. Mater.*, 2011, **23**, 646-657, and references therein.
29. D. Umadevi, S. Panigrahi and G. N. Sastry, *Acc. Chem. Res.*, 2014, **47**, 2574-2581, and references therein.
30. G. Gavrel, B. Jousselme, A. Filoramo and S. Campidelli, *Top. Curr. Chem.*, 2014, **348**, 95-126.
31. R. J. Chen, Y. Zhang, D. Wang and H. Dai, *J. Am. Chem. Soc.*, 2001, **123**, 3838-3839.
32. N. Nakashima, Y. Tomonari and H. Murakami, *Chem. Lett.*, 2002, **31**, 638-639.
33. F. Wang, K. Matsuda, A. F. M. M. Rahman, X. Peng, T. Kimura and N. Komatsu, *J. Am. Chem. Soc.*, 2010, **132**, 10876-10881.
34. K. Umemura, *Nanomaterials*, 2015, **5**, 321-350, and references therein.
35. X. Tu, S. Manohar, A. Jagota and M. Zheng, *Nature*, 2009, **460**, 250-253.
36. S. Iliafar, J. Mittal, D. Vezenov and A. Jagota, *J. Am. Chem. Soc.*, 2014, **136**, 12947-12957.
37. S. G. Stepanian, V. A. Karachevtsev, A. Y. Glamazda, U. Dettlaff-Weglikowska and L. Adamowicz, *Mol. Phys.*, 2003, **101**, 2609-2614.
38. C. Romero-Nieto, R. García, M. Á. Herranz, C. Ehli, M. Ruppert, A. Hirsch, D. M. Guldi and N. Martín, *J. Am. Chem. Soc.*, 2012, **134**, 9183-9192.
39. C. Romero-Nieto, R. García, M. A. Herranz, L. Rodríguez-Pérez, M. Sánchez-Navarro, J. Rojo, N. Martín and D. M. Guldi, *Angew. Chem., Int. Ed.*, 2013, **52**, 10216-10220.
40. A. de Juan, Y. Pouillon, L. Ruiz-González, A. Torres-Pardo, S. Casado, N. Martín, A. Rubio and E. M. Pérez, *Angew. Chem., Int. Ed.*, 2014, **53**, 5394-5400.
41. A. de Juan, M. Mar Bernal and E. M. Pérez, *ChemPlusChem*, 2015, **80**, 1153–1157.
42. A. López-Moreno and E. M. Pérez, *Chem. Commun.*, 2015, **51**, 5421-5424.
43. L. Rodriguez-Pérez, M. A. Herranz and N. Martín, *Chem. Commun.*, 2013, **49**, 3721-3735, and references therein.
44. F. Schedin, A. K. Geim, S. V. Morozov, E. W. Hill, P. Blake, M. I. Katsnelson and K. S. Novoselov, *Nat. Mater.*, 2007, **6**, 652-655.
45. J. A. Mann, J. Rodríguez-López, H. D. Abruña and W. R. Dichtel, *J. Am. Chem. Soc.*, 2011, **133**, 17614-17617.
46. N. V. Kozhemyakina, J. M. Englert, G. Yang, E. Spiecker, C. D. Schmidt, F. Hauke and A. Hirsch, *Adv. Mater.*, 2010, **22**, 5483-5487.
47. F. G. Brunetti, H. Isla, J. Arago, E. Ortí, E. M. Pérez and N. Martín, *Chem. Eur. J.*, 2013, **19**, 9843-9848.
48. M. M. Bernal and E. M. Pérez, *Int. J. Mol. Sci.*, 2015, **16**, 10704-10714.
49. M. A. Petrukhina and L. T. Scott, eds., *Fragments of Fullerenes and Carbon Nanotubes: Designed Synthesis, Unusual Reactions, and Coordination Chemistry*, John Wiley & Sons, 2012.
50. M. Gallego, J. Calbo, J. Arago, R. M. Krick-Calderon, F. H. Liquido, T. Iwamoto, A. K. Greene, E. A. Jackson, E. M. Pérez, E. Ortí, D. M. Guldi, L. T. Scott and N. Martín, *Angew. Chem., Int. Ed.*, 2014, **53**, 2170-2175.